

## Equilibrium Properties of Temporally Asymmetric Hebbian Plasticity

Jonathan Rubin,<sup>1</sup> Daniel D. Lee,<sup>2</sup> and H. Sompolinsky<sup>2,3</sup>

<sup>1</sup>*Department of Mathematics, University of Pittsburgh, Pittsburgh, Pennsylvania 15260*

<sup>2</sup>*Bell Laboratories, Lucent Technologies, Murray Hill, New Jersey 07974*

<sup>3</sup>*Racah Institute of Physics and Center for Neural Computation, Hebrew University, Jerusalem 91904, Israel*  
(Received 25 July 2000)

A theory of temporally asymmetric Hebb rules, which depress or potentiate synapses depending upon whether the postsynaptic cell fires before or after the presynaptic one, is presented. Using the Fokker-Planck formalism, we show that the equilibrium synaptic distribution induced by such rules is highly sensitive to the manner in which bounds on the allowed range of synaptic values are imposed. In a biologically plausible multiplicative model, the synapses in asynchronous networks reach a distribution that is invariant to the firing rates of either the presynaptic or postsynaptic cells. When these cells are temporally correlated, the synaptic strength varies smoothly with the degree and phase of their synchrony.

DOI: 10.1103/PhysRevLett.86.364

PACS numbers: 87.18.Sn, 05.10.Gg, 87.10.+e

Recent experimental evidence indicates that synaptic modification in cortical neurons depends on the precise temporal relation between presynaptic and postsynaptic firing [1,2]. Presynaptic spikes that precede postsynaptic firing lead to synaptic potentiation, while those that follow postsynaptic firing elicit synaptic depression. The temporal window for inducing these changes is on the order of 10 msec. Several recent theoretical studies addressed the potential implications of this temporally asymmetric Hebbian (TAH) synaptic plasticity on learning [3–8]. The present study is motivated by recent work by Abbott and co-workers who applied TAH learning in a large population of excitatory presynaptic cells asynchronously driving a single postsynaptic cell [3]. Their simulations showed that the distribution of synapses converged to a bimodal distribution. The synapses either were almost zero or had values close to their upper limit. Moreover, when the firing rate of the presynaptic cells was increased, the number of strong synapses decreased so that there was very little change in the output rate. Thus, the TAH rule seems to provide a mechanism for keeping the mean output rate invariant. Since Hebb rules are presumed to underlie many developmental and learning processes in neuronal systems, it is important to understand the equilibrium properties of networks with TAH plasticity and how they depend upon the particular implementation of these rules.

In this Letter, we study the TAH rule using Fokker-Planck theory [5,8]. Surprisingly, we find that the behavior of the system depends crucially on how the boundaries on the allowed range of synaptic efficacies are incorporated. In particular, the salient features found in [3] are unique to an additive learning rule in which the magnitude of the update does not explicitly depend on the current value of the synapse. A very different behavior is found with a multiplicative rule where the magnitude of the update decreases as either the upper or lower bounds are approached.

TAH plasticity is described as a change to the synaptic efficacy  $w$  between two cells. A pair of spikes in the input

cell and the output cell, at times  $t_i$  and  $t_o$ , respectively, induces a change in  $w$ :

$$\Delta^\pm w = \pm \lambda f_\pm(w) K(|t_o - t_i|). \quad (1)$$

The weight  $w$  is increased by  $\Delta^+ w$  when  $t_o > t_i$  and decreased by  $\Delta^- w$  when  $t_i > t_o$ . The temporal dependence of the update is defined by the filter  $K$  which for simplicity is taken to be  $K(t) \equiv \exp(-t/\tau)$ . The coefficient  $\lambda$  sets the scale of the synaptic change at each update. The factors  $f_\pm(w)$  determine the relative magnitude of the changes in the positive and negative directions.

We consider two particular examples of these update rules. The first is an additive update rule where the magnitude of the changes is independent of  $w$ , so that

$$f_+ = 1; \quad f_- = \alpha. \quad (2)$$

The parameter  $\alpha > 0$  denotes a possible asymmetry between increasing and decreasing the synaptic efficacy. If the update results in a synaptic weight outside the bounds  $0 < w < 1$ , the weight is clipped to the boundary values. For the second example, which we will call the multiplicative rule,

$$f_+(w) = 1 - w; \quad f_-(w) = \alpha w. \quad (3)$$

This results in a synaptic increase (decrease) whose magnitude scales linearly with the distance to the upper (lower) boundary, similar to the model in [8].

To evaluate the equilibrium properties of these rules, the firing activity in the two cells needs to be specified. We consider the case when the input and output activity are stationary stochastic processes. The firing of the input cell is characterized by an instantaneous rate function  $\nu_i(t) = \sum_{t_i} \delta(t - t_i)$ , where  $t_i$  are the spike times of the input cell with mean rate  $\langle \nu_i \rangle = r_{\text{in}}$ . Similarly, the activity of the output cell is given by  $\nu_o(t) = \sum_{t_o} \delta(t - t_o)$  with mean rate  $r_{\text{out}}$ . The correlation between these two spike trains is described by the normalized time delayed cross-correlation function  $C(t) = \langle \nu_i(t') \nu_o(t' + t) \rangle / r_{\text{in}} r_{\text{out}} - 1$ . Note that, for uncorrelated spike trains,  $C(t) = 0$ .

In the limit of small step sizes ( $\lambda \ll 1$ ), Eq. (1) can be averaged in order to describe the behavior of  $w$  on times of order  $1/\lambda$  as a continuous random walk, similar to the approach in [5,8]. This random walk has a mean drift,

$$v = \left\langle \frac{dw}{dt} \right\rangle = r_{\text{in}} r_{\text{out}} [(f_+ - f_-)\tau + f_+ T_+ - f_- T_-], \quad (4)$$

where the weighted correlation times,  $T_{\pm}$ , are

$$T_{\pm} = \int_0^{\infty} dt K(t) C(\pm t). \quad (5)$$

The first term in Eq. (4) is the contribution from uncorrelated firing activity in the cells and is proportional to  $\tau = \int_0^{\infty} dt K(t)$ . The other terms represent the contribution from the synchrony between the two spike trains and are proportional to  $T_{\pm}$ . The expression for the diffusion constant  $D(w)$  of this random walk is more complex and will be presented elsewhere. Here we note that  $D$  is small since it is proportional to the  $\lambda$ . According to Fokker-Planck theory, the equilibrium density  $P(w)$  can be described as a Gibbs distribution with a plasticity potential  $U(w)$  where in the limit of small  $\lambda$

$$U(w) \equiv -\lambda \log[P(w)] \approx -2 \int_0^w dw' v(w')/D(w'). \quad (6)$$

Thus,  $P(w)$  will be concentrated near the global minima of  $U(w)$ . Depending upon the implementation of the model, the minimum can be located at an interior point where the drift  $v(w)$  vanishes, or at the boundaries  $w = 0$  and  $w = 1$ . To evaluate whether the distribution of  $w$  contains

$$v = \begin{cases} [1 - (1 + \alpha)w]\tau r^2 + r(1 - w)e^{-\Delta t/\tau}, & \Delta t > 0, \\ [1 - (1 + \alpha)w]\tau r^2 - \alpha w r e^{\Delta t/\tau}, & \Delta t < 0. \end{cases} \quad (8)$$

Here the drift depends on  $w$ . It is positive for small  $w$  and becomes negative for large values of  $w$ . In this case,  $U$  has an approximately parabolic shape with a minimum located at  $w = w_0$  where the drift velocity vanishes:

$$w_0 = \begin{cases} 1 - \alpha[1 + \alpha + (\tau r)^{-1}e^{-\Delta t/\tau}]^{-1}, & \Delta t > 0, \\ \{1 + \alpha[1 + (\tau r)^{-1}e^{\Delta t/\tau}]\}^{-1}, & \Delta t < 0. \end{cases} \quad (9)$$

This leads to a distribution  $P(w)$  with a narrow peak at  $w_0$ , as shown in Fig. 2(b). For large values of  $\Delta t$ , the input and output cells are essentially uncorrelated, in which case  $w_0 = 1/(1 + \alpha) \approx 0.5$  for  $\alpha \approx 1$ . For positive  $\Delta t \lesssim 50$  msec, the positive correlation between the two cells gives rise to a mean  $\langle w \rangle > 0.5$  as shown in Fig. 1(b). Conversely, for small negative  $\Delta t$ , the reverse correlation leads to a mean  $\langle w \rangle < 0.5$ . Thus, through this learning rule, the synapse smoothly encodes the temporal phase relationship between the presynaptic and postsynaptic cells. A similar dependence is found when one varies the degree of synchrony between the two cells rather than its phase.

a peak at  $0 < w < 1$  or at the boundaries, the specific form of the correlation function  $C(\pm t)$  needs to be considered.

We first consider the simple example where the spike train  $\{t_i\}$  is a homogeneous Poisson process and the output spike train is a shifted version of the input train, i.e.,  $t_o = t_i + \Delta t$  where  $\Delta t$  is the temporal shift between the two spike trains. In this case,  $r = r_{\text{in}} = r_{\text{out}}$ ,  $C(t) = r^{-1}\delta(t - \Delta t)$ , and  $T_{\pm} = r^{-1}\exp(-|\Delta t|/\tau)\theta(\pm\Delta t)$ , where  $\theta(x) = 1$  if  $x > 0$  and 0 otherwise. For the additive model in Eq. (2), this leads to a net drift:

$$v = \begin{cases} (1 - \alpha)\tau r^2 + r e^{-\Delta t/\tau}, & \Delta t > 0, \\ (1 - \alpha)\tau r^2 - \alpha r e^{\Delta t/\tau}, & \Delta t < 0. \end{cases} \quad (7)$$

Here  $v$  (as well as  $D$ ) is independent of  $w$  and the potential  $U(w) \approx -2vw/D$ . In the limit of small  $\lambda$ , the equilibrium distribution will be a  $\delta$  function centered at 0 when  $v < 0$  and at 1 if  $v > 0$ .

These results are confirmed by the simulations shown in Figs. 1(a) and 2(a), where we have taken  $\alpha = 1.05$  and 0.95. For  $\alpha = 1.05$ , the magnitude of the negative change is slightly larger than the positive one. The mean synapse is zero except when  $0 < \Delta t < \Delta t_0$  with  $\Delta t_0 \approx 50$  msec. In this range, the positive correlation between the input and output cells overcomes the negative bias in the update rule to generate a positive drift so that  $w \approx 1$ . The transition at  $\Delta t_0$  is precisely the point where  $T_+ = (\alpha - 1)\tau$ ; see Eq. (7). This behavior is highly sensitive to whether  $\alpha$  is larger or smaller than 1. For  $\alpha = 0.95$ , the mean synapse is at zero only in the range  $-\Delta t_0 < \Delta t < 0$ , where the negative correlation is larger than the positive bias. Otherwise  $w \approx 1$ .

In contrast, for the multiplicative model the drift velocity is given by

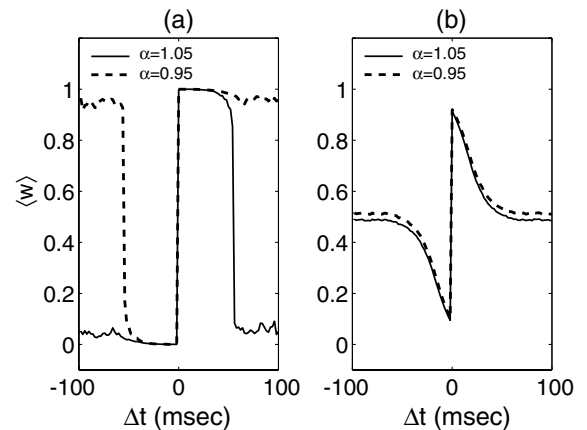


FIG. 1. Simulation results showing the mean synaptic efficacy  $\langle w \rangle$  of a single synapse undergoing (a) additive and (b) multiplicative TAH plasticity.  $\Delta t$  is the time delay imposed on the spike times of the postsynaptic cell relative to those of the presynaptic ones. All simulations are with  $\tau = 10$  msec and  $\lambda = 0.005$ .

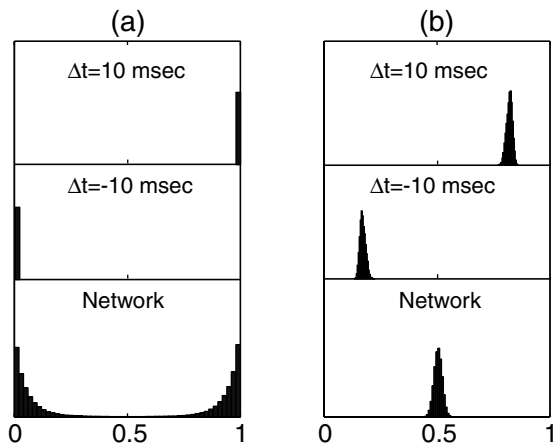


FIG. 2. Histogram showing the distribution of synaptic efficacies using the (a) additive and (b) multiplicative TAH rule with  $\tau = 10$  msec,  $\alpha = 1.05$ ,  $\lambda = 0.005$ . The upper two histograms in each graph show the behavior of a single synapse as described in Fig. 1. The lowest histograms are the distribution of synaptic efficacies in a network of  $N = 1000$  excitatory cells with Poisson activation times and mean input rate  $r_{in} = 10$  Hz. These cells converge on a single integrate and fire cell with parameters  $\tau_m = 20$  msec,  $\tau_s = 5$  msec,  $V_s = 5$ , and  $g_s = 0.01$ .

Let us now consider the situation where a large population of  $N$  cells with modifiable excitatory synapses  $w_i$  drives a single postsynaptic cell. In the numerical simulations below, the output neuron obeys dynamics commonly known as “integrate and fire,” where the potential of the cell is described by the equation  $\tau_m \dot{V} = -V - I_s$ .  $\tau_m$  is the passive time constant of the cell, and when the potential  $V$  reaches the threshold  $V = 1$  it is reset to zero.  $I_s(t)$  is the synaptic current generated by the  $N$  excitatory cells. Each spike in the presynaptic cells triggers a contribution to the output cell’s conductance that decays with synaptic time constant  $\tau_s$ , yielding

$$I_s(t) = g_s \sum_{i=1}^N w_i(t) \sum_{t_i < t} e^{(t-t_i)/\tau_s} (V - V_s). \quad (10)$$

$V_s$  is the reversal potential for the excitatory synapses. The synaptic efficacy  $w_i(t)$  describes the increase in the output cell’s conductance in units of  $g_s$ , immediately after a spike in the  $i$ th cell. The peak conductances,  $w_i$ , are in turn modified by the TAH dynamics described above.

Here we present a general theoretical analysis of the system which is independent of the details of the output cell dynamics. For each  $i$  in the limit of small  $\lambda$ , Eqs. (4)–(6) hold for the  $i$ th synapse, with correlation times  $T_{\pm}^i$  and  $T_{\pm}^i$  defined using the correlation  $C_i(t)$  between the  $i$ th cell and the output. As before, we will assume that the inputs are described by independent homogeneous Poisson processes, all with mean rate  $r_{in}$ . However, the statistics of firing in the output cell are described here by its mean rate  $r_{out}$  and  $\{C_i(t)\}_{i=1}^N$ , determined by its response to the incoming spikes rather than predetermined as in the previous example. We first describe the behavior of the additive model. Because of causality and the Poisson nature of the

input spikes,  $T_-^i = 0$ . For  $T_+^i$ , we make the following plausible assumptions: (i) Since the output cell is driven by a large number of asynchronous inputs,  $T_+^i$  is positive but small; (ii) its value increases roughly linearly with the synaptic efficacy of the  $i$ th presynaptic cell, namely,

$$T_+^i \approx \tau \chi w_i, \quad \chi > 0, \quad (11)$$

where (iii)  $\chi = \chi(r_{out})$  is expected to be a monotonically decreasing function of the firing rate of the output cell.  $\chi$  is larger at smaller  $r_{out}$  when the output cell spends more time near threshold and thus is more sensitive to the timing of the incoming spikes. Equation (11) implies for each synapse the drift  $v_i \propto 1 - \alpha + \chi w_i$ . Thus, if  $\alpha - 1$  is positive and of order 1, the system will converge to a state where all the  $w_i$  are zero, or when  $\alpha < 1$ ,  $w_i \approx 1$ . An interesting situation occurs when  $0 < \alpha - 1 \ll 1$  so that the weak negative bias can balance the weak positive correlations. In this case, the diffusion constant  $D$  is approximately constant, and the potential is given by

$$U(w) \approx \frac{4}{1 + \alpha^2} \left[ (\alpha - 1)w - \frac{1}{2} \chi w^2 \right], \quad (12)$$

which has local minima at the boundaries,  $w = 0, 1$ . This equation has to be solved self-consistently since  $r_{out}$ , which determines  $\chi$ , is itself dependent on  $U$ . Over a wide range of input rates the self-consistent solution is an unsaturated state, in which  $P(w)$  has significant weight both near 0 and near 1, which in turn implies that  $U(0) = U(1)$  up to order  $\lambda$ . Hence by Eq. (12), this state is characterized by an output rate  $r_{out}^*$  such that

$$\chi(r_{out}^*) = 2(\alpha - 1). \quad (13)$$

More precisely, as  $r_{in}$  increases,  $r_{out}$  increases slightly by an amount of order  $\lambda$  inducing a decrease in  $\chi$  of that order. This leads to a small relative increase in  $U(1)$ , which in turn reduces  $P(1)$  by an amount which roughly compensates for the increase in  $r_{in}$ , maintaining Eq. (13). This behavior is confirmed by simulations whose results are shown in Figs. 2(a) and 3(a). As  $r_{in}$  increases from 10 to 40 Hz the output rate remains approximately constant at  $\approx 22$  Hz, and  $\chi \approx 0.1$  in agreement with Eq. (13). The mean efficacy  $\langle w \rangle$  decreases to compensate for the increase in  $r_{in}$ , as found in [3].

The multiplicative model results in a very different state. In fact, since the correlations are weak for large  $N$ , the equilibrium behavior is similar to the previous example with only a single input and output cell with large  $\Delta t$ . In particular, like Eq. (9), the potential  $U(w)$  has a single minimum at the point of zero drift:  $w_0 \approx 1/(1 + \alpha)$ . Thus, the distribution is highly concentrated near  $w_0$ , as seen in Fig. 2(b), and is largely independent of the mean rates of both the input and output cells. As  $r_{in}$  increases, the output rate also increases and is similar in behavior to a cell with fixed synapses,  $w_i \approx w_0$ . Note that, as  $r_{out}$  increases,  $\chi$  decreases but this results in only a small decrease in the mean synaptic efficacy. Finally, in contrast

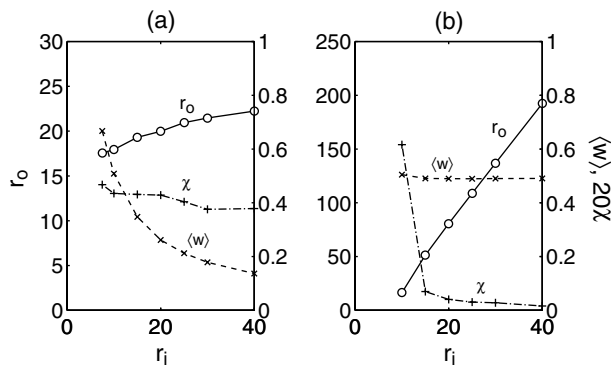


FIG. 3. The effect of increasing the input rate  $r_{in}$  on the equilibrium state of a network of  $N = 1000$  excitatory synapses driving an integrate and fire cell, undergoing (a) additive and (b) multiplicative TAH dynamics. Shown are the output firing rate  $r_{out}$ , the mean synaptic efficacy  $\langle w \rangle$ , and the correlation strength  $\chi$ . The latter was determined by fixing one of the synapses to 0.5 and numerically integrating Eq. (5) and using Eq. (11).

to the additive model where the boundaries are local minima of  $U$  and the point of zero drift is a maximum of  $U$ , in the multiplicative model  $U(w)$  has a single minimum at the point of zero drift. Hence, the equilibration time of the additive model will in general be much slower than that of the multiplicative model since synapses have to overcome the potential barrier of the synaptic potential. Indeed, this difference in equilibration times is seen in our numerical simulations.

We have shown here that the multiplicative TAH rule leads to a very different equilibrium distribution of synapses compared with an additive rule. Most importantly, the multiplicative model is not sensitive to moderate changes in the parameters of the plasticity rule and does not suffer from slow convergence. Furthermore, experimental results reveal a dependence of the magnitudes of the synaptic changes on the amplitude of the initial synaptic efficacy, which supports a multiplicative TAH rule [2]. The observed mean fractional negative change remained constant over a wide range of synaptic efficacies, and is consistent with the assumption that the negative change is proportional to  $w$  as described by a multiplicative  $f_-(w)$  in Eq. (3). The fractional positive changes monotonically decreased with synaptic efficacy and vanished smoothly at some maximum value, again in qualitative agreement with the multiplicative model. Although the observed shape of the  $w$  dependence deviates from the simple linear form of

$f_+(w)$  assumed here, the qualitative properties of the rule are unaffected by this difference. In conclusion, networks combining asynchronous inputs with the multiplicative TAH rule should display an equilibrium synaptic distribution that is largely insensitive to the firing rates of the pre- and postsynaptic cells. On the other hand, a coherent temporal modulation of the firing of the inputs to a target cell leads to a synaptic distribution which encodes the degree and phase of the synchrony between the cells in a smooth manner. It should be noted that the experimentally observed TAH changes set in with a time constant of the order of minutes [1,2], which was not incorporated explicitly in our model. This long time constant may have important implications for dynamic and computational properties of networks. However, this does not appear to affect equilibrium properties, which are the focus of this work.

J. R. is supported in part by the NSF Grant No. DMS-9804447. H. S. is supported in part by a grant of the Israeli Science Foundation and the Israel-U.S.A. Binational Science Foundation. H. S. and D. D. L. acknowledge the support of Bell Laboratories, Lucent Technologies. We thank Mark van Rossum for drawing our attention to a recent work [9] which partially overlaps with this work. We also acknowledge J. Werfel and X. Xie for useful discussions.

- 
- [1] H. Markram *et al.*, *Science* **275**, 213 (1997).
  - [2] G. Q. Bi and M. M. Poo, *J. Neurosci.* **18**, 10464 (1998).
  - [3] L. F. Abbott and S. Song, in *Advances in Neural Information Processing Systems 11*, edited by M. S. Kearns, S. A. Solla, and D. A. Cohn (MIT Press, Cambridge, MA, 1999), pp. 69–75; S. Song, K. D. Miller, and L. F. Abbott (to be published).
  - [4] R. P. N. Rao and T. Sejnowski, in *Advances in Neural Information Processing Systems 12*, edited by S. A. Solla, T. K. Leen, and K.-R. Muller (MIT Press, Cambridge, MA, 2000), pp. 164–170.
  - [5] N. Levy *et al.*, *Advances in Neural Information Processing Systems 12* (Ref. [4]).
  - [6] R. Kempter, W. Gerstner, and J. L. van Hemmen, *Phys. Rev. E* **59**, 4498 (1999).
  - [7] C. W. Eurich *et al.*, *Phys. Rev. Lett.* **82**, 1594 (1999).
  - [8] W. M. Kistler and J. L. van Hemmen, *Neural Comput.* **12**, 385 (2000).
  - [9] M. C. W. van Rossum, G. Q. Bi, and G. G. Turrigiano, *J. Neurosci.* **20**, 8812 (2000).